

Three phase voltage source inverters with grid connected industrial application

Dr. N. Prakash *, V. R. Balaji

Assistant Professor, Department of EEE, Kumaraguru College of Technology, Coimbatore, Tamil Nadu, India

*Corresponding author E-mail: research.prakash77@gmail.com

Abstract

The grid-connected issue is one of the major problems in the field of Power Electronics. In this paper, the Three Phase Voltage Source Inverter (VSI) is controlled by a Space Vector Pulse Width Modulation (SVPWM) Technique. SVPWM control technique and Park transformation, the managed inverter control system to convert input DC power into AC power, stabilize the output voltage and current, and feeds the excess power to the utility grid can be achieved by controllers. Usually, the grid source contains higher level of harmonics. To analyze the harmonics, nonlinear load is connected externally in the point of common coupling. The main aim of this paper is to modeling, simulation and experimental study of the three-phase grid connected inverter. By using the control algorithm, the grid sides Total Harmonics Distortion (THD) are controlled to the 1.54% for 800V DC as per the IEEE standard. The stimulation results such as AC output voltage and current, inverter system power flow, and grid disturbances detection signals, proves the effectiveness of the developed control algorithm. The control algorithms to makes the for this inverter outputs is pure sinusoidal.

Keywords: Grid Connected Inverter; Voltage Source Inverter; Pulse Width Modulation; Space Vector Pulse Width Modulation; AC Power; Grid; Total Harmonics Distortion.

1. Introduction

Fossil fuels and hydropower along with non-commercial fuels such as firewood are considered the main energy resources in India. However, Because of the growing demand in fossil fuel resources and the resulting environmental effects, India's energy strategy aims to increase the reliance on renewable energy sources, particularly wind and concentrated solar power. Consequently, the national energy plan aims to achieve 20% of total generated electricity from renewable energy sources by the year 2020 including 12% from wind energy. This expected to be achieved through establishing grid-connected wind farms and solar Photovoltaic (PV) systems. [1].

Most of renewable energy technology produces a DC power output. An inverter is needed to convert the DC electric energy from the renewable energy source into AC electric energy. The inverters are either stand-alone or grid-connected, In case of grid-connected inverter, the inverter output voltage and frequency should be the same as that of the grid voltage and frequency. Consequently, the control of the inverter should be improved to meet the requirements for grid interconnection. [2].

It is stated that the control tasks of the grid-connected inverter can be divided into two parts: Input-side controller and Grid-side controller. The control objective on the Input-side controller is to capture maximum power from the input source. However, the control objectives on the Grid-side controller are to control the power delivered to the grid, ensure high quality of the injected power and Grid synchronization. [3].

A number of researchers deal with control of the grid side inverter, which use current control loop to regulate the grid current. In other works, the control of the grid-connected inverter is based on two cascaded loops: an internal current loop, which regulates the grid

current, [4] and an external voltage loop, which is designed for balancing the power flow in the system. Moreover, control strategies employing an outer power controller and an inner current control loop are also reported.

In this paper, a comprehensive study of a three-phase grid-connected inverter with grid side controller is presented. To carry this out, the whole inverter system is modelled and simulated using MATLAB simulation package, while taking into consideration the non-ideal behaviour of the constituting elements of the inverter. In addition, the practical implementation is provided to verify the simulation results. Three phases Grid Side Converter consists of the control theory of the grid-side inverter. In addition, the space vector modulation SVM is presented. Moreover, it explains the synchronization method for grid-connected power inverters. [5].

Energy transfer from renewable energy sources to the grid is realized with power electronic converters. Depending on the energy source, different power converters can be utilized in Distributed Power Generation Systems (DPGSs). DC energy produced by PV panels or fuel cells is generally converted to constant DC voltage with DC/DC converter which provides DC-link of the inverter. In case of wind power systems, [6] the DC-link voltage is obtained with an AC/DC converter. In some applications, an additional DC/DC converter can be used to boost the DC voltage. In the last stage, an inverter converts the DC energy to AC energy in order to transfer the energy from DC-link to the grid.

[7] In grid connected systems, two basic considerations are THD value of grid current and the power factor of the generated power. The THD value of grid current is required to be less than 5%. Three-phase currents must be synchronized with related three-phase voltages. In order to satisfy the power quality standards, inverter control and modulation technique have an important role. Three-phase inverters can be controlled in synchronous rotating

frame (d-q), stationary reference frame ($\alpha\beta$) and natural frame (a-b-c).[8] In d-q frame control, three-phase voltages and currents are transformed by Park transformation into the d-q reference frame that rotates synchronously with the grid voltage. Thus, three-phase variables become DC quantities. As the control variables are DC, different filtering methods can be used, and PI controller achieves good performance in this reference frame control. In stationary reference frame, three-phase quantities are transformed into $\alpha\beta$ frame by Clarke transformation. Thus the variables become sinusoidal. PI controller cannot regulate the current well; therefore the current has a steady-state error. PR controller is the most common controller in stationary reference frame. As PR controller is used with $\alpha\beta$ quantities, [9] Park transformation can be avoided. The natural reference frame control uses the three-phase grid voltages and currents. Hence, each phase value can be controlled individually. Hysteresis Current Control (HCC) and linear current control techniques are widely used in stationary reference frame control.

[10] In three-phase grid connected inverters, the most commonly used modulation technique is Space Vector Pulse Width Modulation (SVPWM). This technique controls output voltage vector of inverter and provides optimum switching pattern. Optimum switching decreases the switching frequency and switching losses. The other advantages of SVPWM technique are constant switching frequency, low harmonic content and better DC-link voltage utilization than the conventional sine PWM.

2. Three phase voltage source inverters

[11] In order to control three-phase Voltage-Source Inverters (VSI), there are two control strategies: current control and voltage control. The voltage-controlled VSI use the phase angle between the inverter output voltage and the grid voltage to control the power flow. In the current controlled VSI, the active and reactive components of the current injected into the grid are controlled using Pulse Width Modulation (PWM) techniques.

A current controller is less sensitive to voltage phase shifts and to distortion in the grid voltage. Moreover, it is faster in response. On the other hand, the voltage control is sensitive to small phase errors and large harmonic currents may occur if the grid voltage is distorted. Consequently, the current control is recommended in the control of grid-connected inverter.

a) Block Diagram

The block diagram of the three-phase grid connected inverter system is shown in Fig.1. The DC-link voltage is obtained from three-phase grid with a transformer, a diode rectifier and capacitors. The transformer boosts the voltage and high DC-link voltage is obtained. [12], [13]

The three-phase two-level IGBT Intelligent Power Module (IPM) inverter is connected to the grid through L filters. The inverter is controlled with FPGA control board.

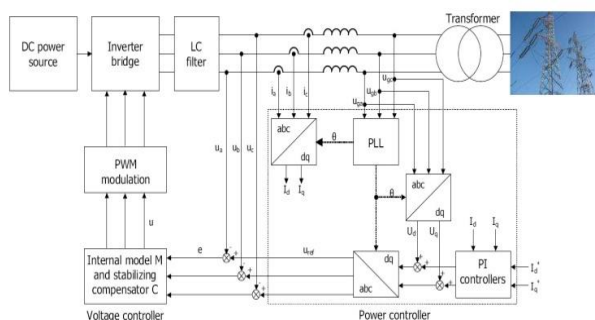


Fig. 1: Block Diagram of the Grid Connected Inverter.

b) Theory of the Three-Phase Grid-Connected Inverter

The current controller of three-phase VSI plays an essential part in controlling grid-connected inverters. Consequently, the quality of the applied current controller largely influences the performance of the inverter system.

Many control mechanisms have been proposed to regulate the inverter output current that is injected into the utility grid. Among these control mechanisms, three major types of current controller have evolved: hysteresis controller, predictive controller and linear Proportional-Integral (PI) controller.

Predictive controller has a very good steady-state performance and provides a good dynamic performance. However, its performance is sensitive to system parameters. The hysteresis controller has a fast transient response, non-complex implementation and an inherent current protection.

However, the hysteresis controller has some drawbacks such as variable switching frequency and high current ripples. These cause a poor current quality and introduce difficulties in the output filter design.

The main objective of static power converters is to produce an AC output waveform from a DC power supply. These are the types of waveforms required in Adjustable Speed Drives (ASDs), Uninterruptible Power Supplies (UPS), static VAR compensators, active filters, Flexible AC Transmission Systems (FACTS), and voltage compensators, which are only a few applications. For sinusoidal ac outputs, the magnitude, frequency, and phase should be controllable. [14]

According to the type of ac output waveform, these topologies can be considered as Voltage Source Inverters (VSIs), where the independently controlled ac output is a voltage waveform. [15] These structures are the most widely used because they naturally behave as voltage sources as required by many industrial applications, such as Adjustable Speed Drives (ASDs), which are the most popular application of inverters. Similarly, these topologies can be found as Current Source Inverters (CSIs), where the independently controlled ac output is a current waveform.

These structures are still widely used in medium-voltage industrial applications, where high-quality voltage waveforms are required. Static power converters, specifically inverters, are constructed from power switches and the ac output waveforms are therefore made up of discrete values. This leads to the generation of waveforms that feature fast transitions rather than smooth ones.[16]

For instance, the ac output voltage produced by the VSI of a standard ASD is a three-level waveform. Although this waveform is not sinusoidal as expected, its fundamental component behaves as such. This behaviour should be ensured by a modulating technique that controls the amount of time and the sequence used to switch the power valves on and off. The modulating techniques most used are the carrier-based technique (e.g., Sinusoidal Pulse Width Modulation (SPWM)), the Space-Vector (SV) technique, and the Selective-Harmonic-Elimination (SHE) technique.

c) Operation of Three Voltage Inverter

[17] Single-phase VSIs cover low-range power applications and three-phase VSIs cover the medium- to high-power applications. The main purpose of these topologies is to provide a three-phase voltage source, where the amplitude, phase, and frequency of the voltages should always be controllable. Although most of the applications require sinusoidal voltage waveforms (e.g., ASDs, UPSs, FACTS, VAR compensators), arbitrary voltages are also required in some emerging applications (e.g., active filters, voltage compensators).

The standard three-phase VSI topology is shown in Fig. 2 and the eight valid switch states are given in Table 1. As in single-phase VSIs, the switches of any leg of the inverter (S_1 and S_4 , S_3 and S_6 , or S_5 and S_2) cannot be switched on simultaneously because this would result in a short circuit across the DC link voltage supply. Similarly, in order to avoid undefined states in the VSI, and thus undefined AC output line voltages, the switches of any leg of the inverter cannot be switched off simultaneously as this will result in voltages that will depend upon the respective line current polarity. Of the eight valid states, two of them (7 and 8 in Table 1) produce zero AC line voltages.

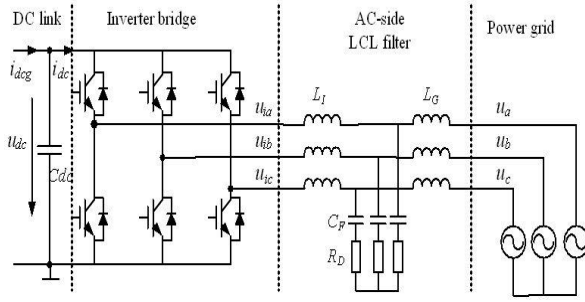


Fig. 2: Three Phase Voltage Source Inverter.

In this case, the ac line currents freewheel through either the upper or lower components. The remaining states (1 to 6 in Table 3.1) produce non-zero ac output voltages. In order to generate a given voltage waveform, the inverter moves from one state to another. Thus the resulting AC output line voltages consist of discrete values of voltages that are V_i , 0, and $-V_i$ for the topology shown in Fig. 2. The selection of the states in order to generate the given waveform is done by the modulating technique that should ensure the use of only the valid states.

Table 1: Switch States for a Full-Bridge Three-Phase VSI

State	State	V_{ab}	V_b	V_a	Space Vector
2,6 ON 4,5,3 OFF	1	v	0	$-v$	$V_1=1+j0.5$
3,1 ON 4,5,6 OFF	2	0	v	$-v$	$V_2=j1.55$
4,2 ON 1,5,6 OFF	3	$-v$	v	0	$V_3=-1+j0.5$
5,3 ON 1,2,6 OFF	4	$-v$	0	v	$V_4=-1-j0.5$
6,4 ON 1,2,3 OFF	5	0	$-v$	v	$V_5=j1.55$
1,5 ON 2,3,4 OFF	6	v	$-v$	0	$V_6=1-j0.5$
3,5 ON 2,4,6 OFF	7	0	0	0	$V_7=0$
6,2 ON 1,3,5 OFF	8	0	0	0	$V_8=0$

3. Design of the inverter

The control block diagram of the system is shown in Fig.3. The grid voltages are measured, and grid angle is determined with PLL method. The grid angle is used to transform the grid currents and voltages from a-b-c reference frame to d-q reference frame by Park transformation as given in Eqn. (1). The error is calculated from the reference and measured d-q currents, and the errors in d-q frame are given to PI regulators.

The reference d-component of the current defines the maximum value of the grid current. The q-component current controls the reactive power flow. It is set to zero for only active power injection. PI outputs are summed with feed-forward grid voltage components and decoupling components to produce reference inverter output voltages.

The outputs of the PI regulators are transformed into α - β frame using Eqn. (2). Inverter reference voltages in α - β reference frame and DC-link voltage are used in the SVPWM, and the switching signals are produced. [18], [19].

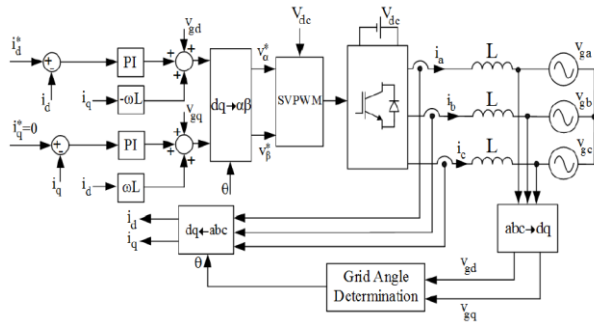


Fig. 3: Control Block Diagram of the Inverter.

$$\begin{pmatrix} v_d \\ v_q \end{pmatrix} = \frac{2}{3} \begin{bmatrix} \cos \theta & \cos(\theta - \frac{2\pi}{3}) & \cos(\theta - \frac{4\pi}{3}) \\ -\sin \theta & \sin(\theta - \frac{2\pi}{3}) & -\sin(\theta - \frac{2\pi}{3}) \end{bmatrix} \begin{pmatrix} V_a \\ V_b \\ V_c \end{pmatrix} \quad (1)$$

$$\begin{pmatrix} v_\alpha \\ v_\beta \end{pmatrix} = \begin{pmatrix} \cos \theta & -\sin \theta \\ \sin \theta & \cos \theta \end{pmatrix} \quad (2)$$

The sector changes in each 60° , therefore the sector of reference vector is determined according to the calculated vector angle. The inverter produces the voltage with combination of two adjacent vectors and zero vectors.

The phase angle of grid voltage is calculated by software PLL. The algorithm block diagram is given in Fig. 4. Grid angle is calculated using the q-component of grid voltage. The reference value of angle is set to zero. Angle error is given to PI regulator, and it generates angular frequency.

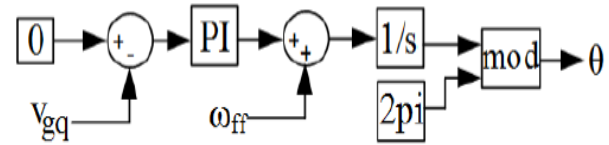


Fig. 4: PLL Algorithm Block Diagram.

The output signal of PI is added to fundamental angular frequency of grid voltage to calculate the actual angular frequency. Instantaneous phase angle is obtained by integrating the angular frequency. Phase angle variation with phase-a grid voltage is seen in Fig. 5.

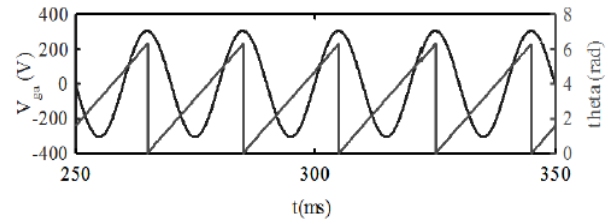


Fig. 5: Grid Angle Variations.

a) Modeling of System

The circuit topology that is modelled for parametric analysis is shown in Fig. 6. It is assumed that three-phase grid voltages are balanced and stable, the switches are ideal, and DC-link voltage is constant. The system can be modelled in different frames such as d-q, α - β and a-b-c. d-q model of the system is given in Eqn. (3).

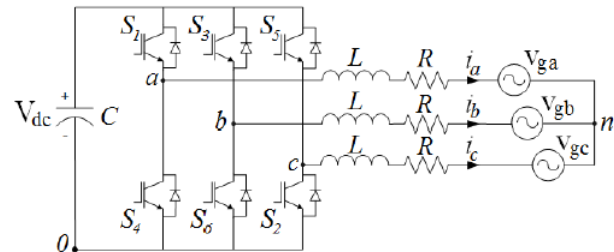


Fig. 6: Three-Phase Grid Connected Inverter.

$$v_d = L \frac{di_d}{dt} - \omega L i_q + v_{gd} \quad (3)$$

$$v_q = L \frac{di_q}{dt} - \omega L i_d + v_{gq} \quad (4)$$

Where, v_d and v_q are inverter output voltages, i_d and i_q are grid currents, v_{gd} and v_{gq} are grid voltages, ω is grid frequency and L is inverter output filter inductance. In this study, the system is modelled in a-b-c reference frame as given in Eqn. (5-7). R is the Equivalent Series Resistance (ESR) value of the inductance.

The circuit equation for each phase can be derived as seen in Eqn. (5). Since the inverter has three-wire, there is a voltage difference (v_{no}) between neutral point of the grid and negative point of the DC-link. The v_{no} is defined as a function of inverter output voltages by Eqn. (6), and the inverter output voltages are defined as a function of leg switching states by Eqn. (7),

$$V_{ko} = L \frac{di_k}{dt} + Ri_k + V_{gk} + V_{no} \quad (5)$$

$$V_{no} = \frac{1}{3}(V_{ao} + V_{bo} + V_{co}) \quad (6)$$

$$V_{ko} = S_k \cdot V_{dc} = \begin{cases} V_{dc}, & S_k = 1 \\ 0, & S_k = 0 \end{cases} \quad (7)$$

In the equations above, k represents the phase of inverter, $k \in \{a, b, c\}$ and S defines the states of upper switches. When S is 1, the related upper switch is ON and lower switch is OFF in the inverter leg. Eqn. (9) and (10), the model of the grid connected inverter can be written in the state-space equation as below,

$$\dot{x} = Ax + Bu \quad (8)$$

$$y = Cx \quad (9)$$

The state and input vectors can be defined by Eqn. (10) and Eqn. (11), respectively.

$$x = [i_a \quad i_b \quad i_c]^T \quad (10)$$

$$u = \begin{pmatrix} V_{ao} - V_{ga} - V_{no} \\ V_{bo} - V_{gb} - V_{no} \\ V_{co} - V_{gc} - V_{no} \end{pmatrix} \quad (11)$$

b) Grid Synchronization

The inverter output current that is injected into the utility network must be synchronized with the grid voltage. The objective of the synchronization algorithm is to extract the phase angle of the grid voltage. The feedback variables can be converted into a suitable reference frame using the extracted grid angle. Hence, the detection of the grid angle plays an essential role in the control of the grid-connected inverter. The synchronization algorithms should respond quickly to changes in the utility grid. Moreover, they should have the ability to reject noise and the higher order harmonics. Many synchronization algorithms have been proposed to extract the phase angle of the grid voltage such as zero crossing detection, and Phase-Locked Loop (PLL).

The simplest synchronization algorithm is the zero crossing detection. However, this method has many disadvantages such as low dynamics. In addition, it is affected by noise and higher order harmonics in the utility grid. Therefore, this method is unsuitable for applications that require consistently accurate phase angle detection. [20].

Nowadays, the most common synchronization algorithm for extracting the phase angle of the grid voltages is the PLL. The PLL can successfully detect the phase angle of the grid voltage even in the presence of noise or higher order harmonics in the grid. [21]

A controller, usually FPGA, is used to control this variable, which brings the phase error to zero and acts as a loop filter. The ω_{ref} represents the utility nominal frequency that is added to the output of the regulator then outputted as the grid frequency. After the loop filter, whose output is the grid frequency, a Voltage-Controlled Oscillator (VCO) is applied. This is usually an integrator, which gives the phase locked angle of the grid θ as output.

4. Simulation results

The Three Phase grid connected Inverter is as shown in the Fig. 7 and the Input voltage of the inverter is set as 900V and the IGBT Switch is used for the Inverter.

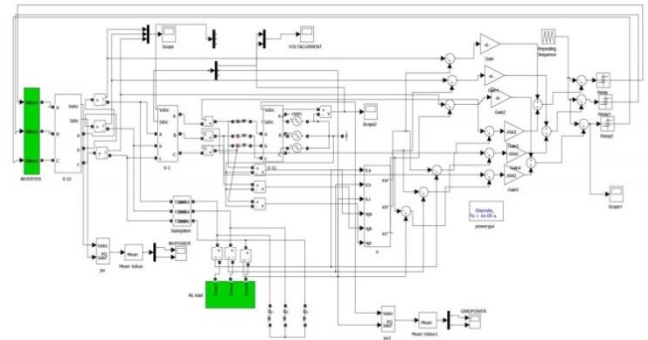


Fig. 7: Simulation Diagram of Grid Connected Three Phase Inverter.

5. Simulation parameters

The simulation of normal three phase Inverter circuit diagram is as shown in Fig. 7 and the simulation parameters values are tabulated in Table 2.

Table 2: Simulation Parameters

Input Voltage	900V
Switch	IGBT
Internal Resistance	0.001
Snubber Resistance	1e5
Grid Voltage	325V
Frequency	50Hz

The input voltage of the inverter is set as 900V it is shown in the Fig. 8 and the grid side voltage is set as 325V, it is shown in the Fig. 9. Grid side Voltage and current waveform is as shown in Fig. 10 and the grid power is as shown in Fig. 11.

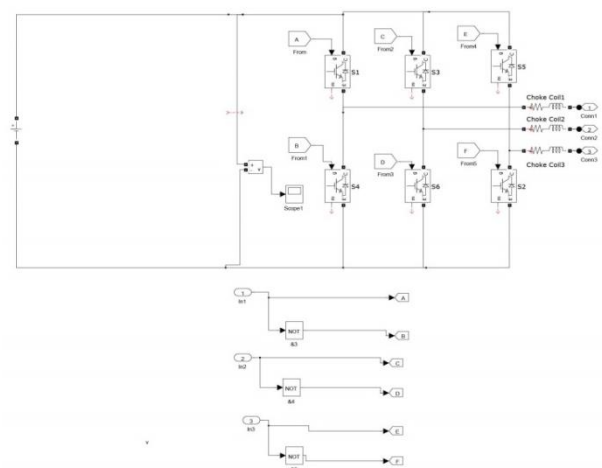


Fig. 8: Simulation of Three Phase Inverter.

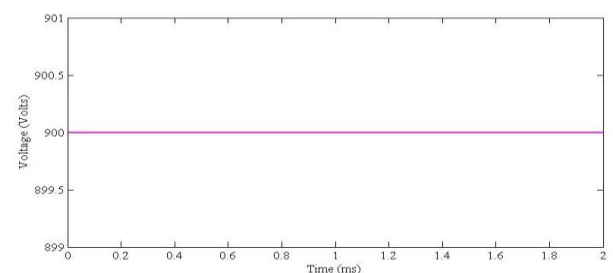


Fig. 9: Input Voltage of the Inverter.

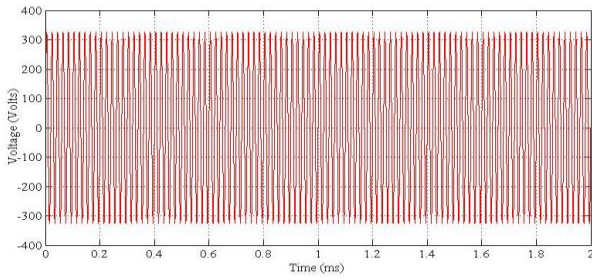


Fig. 10: Grid Side Voltage.

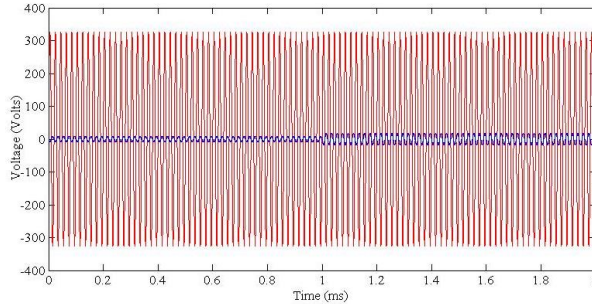


Fig. 11: Grid Voltages and Current.

Grid side Voltage and current waveform is as shown in Fig. 11 and the grid power is as shown in Fig. 12. Grid side Voltage and current waveform is as shown in Fig. 13 and the grid power is as shown in Fig. 14. The output value Parameters are tabulated in Table 3.

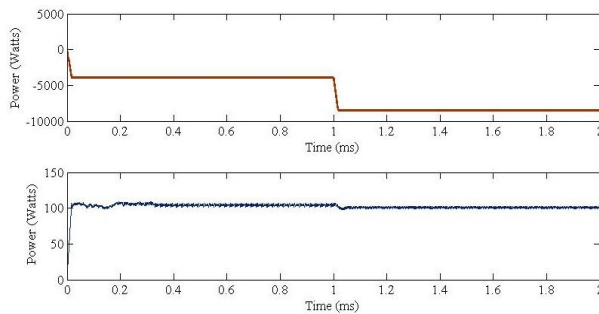


Fig. 12: Grid side Real and Reactive Power.

Table 3: Output Parameter Comparison

Input DC Voltage	900V
Grid Voltage	325 V
Grid Power	-5000 to -10000W
Inverter Power	5000 to 10000W

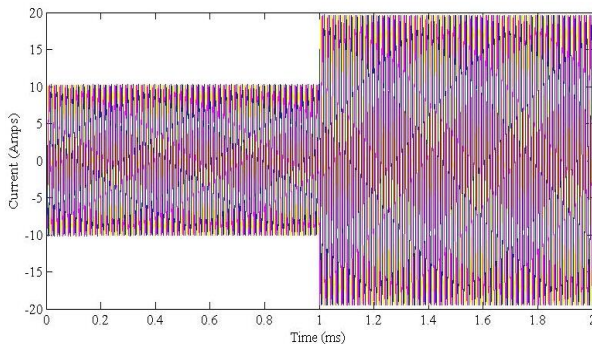


Fig. 13: Inverter Current.

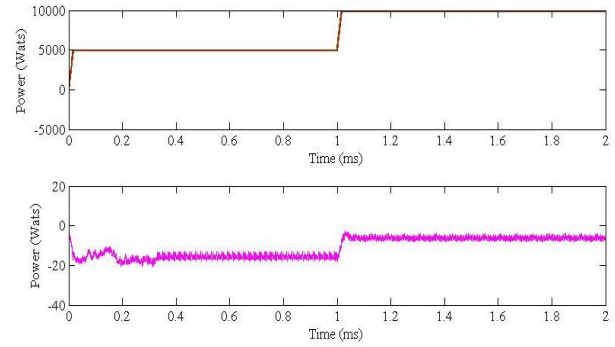


Fig. 14: Inverter Real and Reactive Powers.

THD measurement of input 900V DC voltage is as shown in Fig. 15 and the THD measurement of input 1000V DC voltage is as shown in below.

THD value of different PWM is shown in Fig. 16. The THD measurement of different input voltage is tabulated in Table 3.

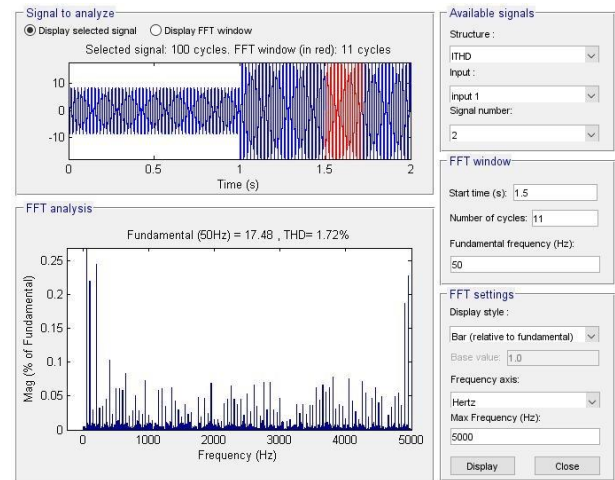


Fig. 15: THD Measurement of Input 900 V DC Voltage.

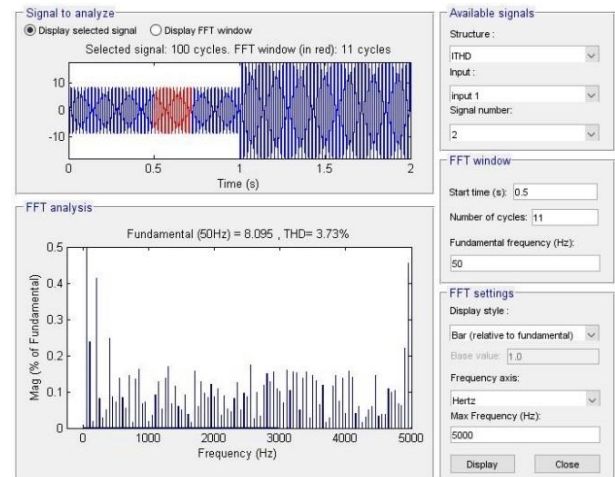


Fig. 16: THD Measurement of Input 1000 V DC Voltage.

6. Conclusion

Grid connected Three Phase Voltage Source Inverter (VSI) has been successfully designed and simulated by using MATLAB Simulink. The simulation parameters and various waveforms have been obtained. The obtained result clearly reflects that the designed three phase VSI have reduced the harmonics as per IEEE standard. The THD measurements are taken for various input voltages and the corresponding results are plotted as well as tabulated. These results are shown the grid side harmonics are always within the limit, which is less than 5% (IEEE standard). The developed

control algorithm for this inverter makes the output signal is pure sinusoidal.

References

- [1] Balasubramanian K., and John V., (2015), 'Thermal test method for high power three-phase grid-connected inverters,' in *IET Power Electronics*, Vol. 8, No. 9, pp. 1670-1680. <https://doi.org/10.1049/iet-pel.2014.0152>.
- [2] Chen Y. and Smedley K. M., (2008), 'One-Cycle-Controlled Three-Phase Grid-Connected Inverters and Their Parallel Operation,' in *IEEE Transactions on Industry Applications*, vol. 44, no. 2, pp. 663-671. <https://doi.org/10.1109/TIA.2008.916718>.
- [3] Chen D., Jiang J., Qiu Y., Zhang J., and Huang F., (2017), 'Single-Stage Three-Phase Current-Source Photovoltaic Grid-Connected Inverter High Voltage Transmission Ratio,' in *IEEE Transactions on Power Electronics*, Vol. 32, No. 10, pp. 7591-7601. <https://doi.org/10.1109/TPEL.2016.2622722>.
- [4] Chen Y., and Smedley K., (2008) 'Three-Phase Boost-Type Grid-Connected Inverter,' in *IEEE Transactions on Power Electronics*, Vol. 23, No. 5, pp. 2301-2309. <https://doi.org/10.1109/TPEL.2008.2003025>.
- [5] El-Naggar and Erlich I., (2016), 'Control approach of three-phase grid connected PV inverters for voltage unbalance mitigation in low-voltage distribution grids,' in *IET Renewable Power Generation*, Vol. 10, No. 10, pp. 1577-1586. <https://doi.org/10.1049/iet-rpg.2016.0200>.
- [6] He Y., Chung H. S. h., Ho C. N. M., and Wu W., (2017), 'Direct Current Tracking Using Boundary Control With Second-Order Switching Surface for Three-Phase Three-Wire Grid-Connected Inverter,' in *IEEE Transactions on Power Electronics*, Vol. 32, No. 7, pp. 5723-5740. <https://doi.org/10.1109/TPEL.2016.2608355>.
- [7] Han G., Xia Y., and Min W., (2012), 'Study on the three-phase PV grid-connected inverter based on deadbeat control,' *2012 Power Engineering and Automation Conference*, Wuhan, pp. 1-4.
- [8] He Y., Chung H. S. H., Ho C. N. M., and Wu W., (2017) 'Modified Cascaded Boundary-Deadbeat Control for a Virtually-Grounded Three-Phase Grid-Connected Inverter with LCL Filter,' in *IEEE Transactions on Power Electronics*, Vol. 32, No. 10, pp. 8163-8180. <https://doi.org/10.1109/TPEL.2016.2637078>.
- [9] Hintz O., Prasanna U. R., and Rajashekara K., (2016), 'Comparative Study of the Three-Phase Grid-Connected Inverter Sharing Unbalanced Three-Phase and/or Single-Phase systems,' in *IEEE Transactions on Industry Applications*, Vol. 52, No. 6, pp. 5156-5164, Nov.-Dec. 2016. <https://doi.org/10.1109/TIA.2016.2593680>.
- [10] Lee K. J., Park B. G., Kim R. Y. and Hyun D. S., (2012), 'Robust Predictive Current Controller Based on a Disturbance Estimator in a Three-Phase Grid-Connected Inverter,' in *IEEE Transactions on Power Electronics*, Vol. 27, No. 1, pp. 276-283, Jan. 2012. <https://doi.org/10.1109/TPEL.2011.2157706>.
- [11] Liu J., Zhou L., Yu X., Li B., and Zheng C., (2017), 'Design and analysis of an LCL circuit-based three-phase grid-connected inverter,' in *IET Power Electronics*, Vol. 10, No. 2, pp. 232-239, 2 10 2017.
- [12] Thanh-Vu Tran, Tae-Won Chun, Hong-Hee Lee, Heung-Geun Kim and Eui-Cheol Nho, (2012), 'Control for grid-connected and stand-alone operations of three-phase grid-connected inverter,' *2012 International Conference on Renewable Energy Research and Applications (ICRERA)*, Nagasaki, pp. 1-5. <https://doi.org/10.1109/ICRERA.2012.6477348>.
- [13] Baskar, S., Pavithra, S., & Vanitha, T. (2015, February). Optimized placement and routing algorithm for ISCAS-85 circuit. In *Electronics and Communication Systems (ICECS), 2015 2nd International Conference on* (pp. 958-964). IEEE.
- [14] Baskar, S., & Dhulipala, V. S. RELIABILITY ORIENTED PLACEMENT AND ROUTING ANALYSIS IN DESIGNING LOW POWER MULTIPLIERS.
- [15] Chandra, M. E. H., & Scholar, P. G. (2014). ENHANCED DECODING ALGORITHM FOR ERROR DETECTION AND CORRECTION IN SRAM.
- [16] Maheswari, M. U., Baskar, S., & Keerthi, G. M. High Speed Finite Field Multiplier GF (2 M) for Cryptographic Applications.
- [17] Raghupathi, S., & Baskar, S. (2012). Design and Implementation of an Efficient and Modernised Technique of a Car Automation using Spartan-3 FPGA. *Artificial Intelligent Systems and Machine Learning*, 4(10).
- [18] Moreno J. C., Espi Huerta J. M., Gil R. G., and Gonzalez S. A., (2009), 'A Robust Predictive Current Control for Three-Phase Grid-Connected Inverters,' in *IEEE Transactions on Industrial Electronics*, Vol. 56, No. 6, pp. 1993-2004, June 2009. <https://doi.org/10.1109/TIE.2009.2016513>.
- [19] Qiu Y., Xiao L., Zhang N., and Yao Z., (2011), 'Stability of three-phase grid-connected inverters,' *Proceedings of the 2011 14th European Conference on Power Electronics and Applications*, Birmingham, pp. 1-9.
- [20] Wang Z., Chang and L., (2007), 'A Novel V_{dc} Voltage Monitoring and Control Method for Three-Phase Grid-Connected Inverter,' *2007 IEEE Power Electronics Specialists Conference*, Orlando, FL, pp. 1221-1226. <https://doi.org/10.1109/PESC.2007.4342167>.
- [21] Wang Z., Chang L., and Mao M., (2010), 'DC voltage sensorless control method for three-phase grid-connected inverters,' in *IET Power Electronics*, Vol. 3, No. 4, pp. 552-558. <https://doi.org/10.1049/iet-pel.2008.0282>.